Research Article

Theophylline Cocrystals Prepared by Spray Drying: Physicochemical Properties and Aerosolization Performance

Amjad Alhalaweh,[1] Waseem Kaialy,[1,2,3] Graham Buckton,[4] Hardyal Gill,[3] Ali Nokhodchi,[2] and Sitaram P. Velaga[1,5]

Abstract. The purpose of this work was to characterize theophylline (THF) cocrystals prepared by spray drying in terms of the physicochemical properties and inhalation performance when aerosolized from a dry powder inhaler. Cocrystals of theophylline with urea (THF-URE), saccharin (THF-SAC) and nico-tinamide (THF-NIC) were prepared by spray drying. Milled THF and THF-SAC cocrystals were also used for comparison. The physical purity, particle size, particle morphology and surface energy of the materials were determined. The *in vitro* aerosol performance of the spray-dried cocrystals, drug-alone and a drug-carrier aerosol, was assessed. The spray-dried particles had different size distributions, morphologies and surface energies. The milled samples had higher surface energy than those prepared by spray drying. Good agreement was observed between multi-stage liquid impinger and next-generation impactor in terms of assessing spray-dried THF particles. The fine particle fractions of both formulations were similar for THF, but drug-alone formulations outperformed drug-carrier formulations for the THF cocrystals. The aerosolization performance of different THF cocrystals was within the following rank order as obtained from both drug-alone and drug-carrier formulations: THF-NIC>THF-URE>THF-SAC. It was proposed that micromeritic properties dominate over particle surface energy in terms of determining the aerosol performance of THF cocrystals. Spray drying could be a potential technique for preparing cocrystals with modified physical properties.

KEY WORDS: aerodynamic diameter; cocrystal; spray drying; surface energy; theophylline.

INTRODUCTION

Engineering pharmaceutical materials for pulmonary delivery involves the design of particles with good dispersibility to aid lung deposition. The dispersion of the inhaled particles depends on the aerodynamic stress and particle aggregate strength, in addition to many other interdependent factors such as particle morphology, size, density, *etc.* (1–5). The strength of an aggregate depends on the cohesive and adhesive interactions, such as van der Waals, electrostatic and capillary forces, which are in turn dependent on the surface chemistry or solid-state nature of the material and the external environment (6).

[1] Pharmaceutical Materials Research Group, Department of Health Science, Luleå University of Technology, Luleå, 971 87, Sweden.
[2] Chemistry and Drug Delivery Group, Medway School of Pharmacy, University of Kent, ME4 4TB, Kent, UK.
[3] Pharmaceutics and Pharmaceutical Technology Department, University of Damascus, Damascus, Syria.
[4] Department of Pharmaceutics, School of Pharmacy, University College London, 29-39 Brunswick Square, London, WC1N 1AX, UK.
[5] To whom correspondence should be addressed. (e-mail: sitvel@ltu.se)

Surface energy (γ) can be divided into polar and nonpolar (dispersive) components (7,8). The polar part can be further sub-divided into acid and base components (9). Several approaches have been used to measure the surface energy of powders. The liquid and vapour probe techniques, contact angle and inverse gas chromatography (IGC), respectively, are probably the most popular choices (10,11). Different methods of measurement could result in varied surface energy values for a specific material (12). Nonetheless, some studies have reported good correlations between these methods for the surface energy of particles (13,14). IGC is a potentially interesting technique for investigating the surface properties of pharmaceutical materials (11). The theory behind surface energy measurements using IGC has been described in detail in many articles; the main equations are elaborated in the later section (11,15).

In general, amorphous powders have a higher surface free energy than crystalline material, which makes crystalline material a more favourable choice for drug formulations (16). However, crystalline solids can be poorly soluble, thus negatively affecting drug dissolution and bioavailability characteristics. In recent years, the formation of cocrystals (crystalline solid forms composed of a drug and a conformer) has been shown to improve the physiochemical properties, such as solubility, dissolution, stability, mechanical properties and bioavailability, of drug molecules (17–19). The formation of cocrystals can also alter the bulk as well as surface properties

of the drug, potentially resulting in superior performance of the engineered materials. The availability of several cocrystal formers provides enormous flexibility for crystal engineering and fine-tuning of the particle surface properties for different applications. While a number of studies have been dedicated to the screening, formation and scale-up of cocrystals, only a few have related their material properties to their performance (20–25). It was shown using atomic force microscope that the interaction of moisture with caffeine cocrystals is different due to the difference in the crystal structures (26).

Milling and spray drying are widely used particle processing techniques in the pharmaceutical industry. While milling is a standard method for particle-size reduction, spray drying is an efficient technique for engineering particles for different applications, including delivery by inhalation (27), and has been shown to be a suitable method for preparing cocrystals (28).

Theophylline (THF) is a bronchodilator used for treating asthma, breathing difficulties, *etc.* Its solid-state chemistry and its phase transformation behaviour in the solid state and in water have been widely studied (29–31). THF exists in four polymorphic forms (I, II, III and IV) and a hydrate (29,30,32). THF form I is the stable polymorph at room temperature; the hydrated form is stable in water. Several cocrystals of theophylline (about 20) have been identified (33).

The purposes of this study were to: (1) use spray drying as a method to prepare cocrystal particles of THF, (2) study the impact of different cocrystals form of THF on particulate properties and inhalation performance and (3) investigate the impact of different processes on particulate and bulk properties.

THF cocrystals with diverse conformers were used as model drugs (34–36). THF cocrystals were prepared by spray drying. The solid-state purity, particle morphology and size of the cocrystals were examined pre- and post-processing. In addition, the surface energy of the materials was measured using IGC. The *in vitro* aerosol behaviour of the spray-dried cocrystals was studied using dry powder aerosols containing the drug-alone and a drug-carrier aerosol. This study demonstrates the potential of using cocrystal solid forms prepared by spray drying for pulmonary drug delivery.

MATERIALS AND METHODS

Materials

All chemicals and solvents were purchased from Sigma-Aldrich (Stockholm, Sweden) and used as received. Milli-Q water was used in the study. α-Lactose monohydrate was sourced from DMV International, The Netherlands.

Saturation Condition Determination

The saturation condition (incongruently saturating or congruently saturating) of cocrystals in the solvents used was investigated by slurring a stoichiometric mixture of drug and coformer. A detailed description of the theory on cocrystal saturation condition and experimental procedures is provided in our previous article (28). Briefly, congruently saturating cocrystals are thermodynamically stable during slurring and can be readily formed by slurring the stoichiometric ratio of cocrystal components. On the other hand, incongruently saturating cocrystals transform during slurring, resulting in a less soluble solid

form. The final powder was analysed by differential scanning calorimetry (DSC) or/and powder x-ray diffraction (PXRD).

Preparation of Cocrystals by Spray Drying

Cocrystals of THF with urea (THF-URE), saccharin (THF-SAC) and nicotinamide (THF-NIC) were prepared by spray drying. The various solvents and solution concentrations used in spray drying are listed in Table I. The organic solutions were spray dried in a closed configuration with nitrogen as the drying gas. The solvent was trapped using a B-295 inert loop. The aqueous solutions were spray dried in an open configuration with air as the drying gas. The processing conditions were: air flow 357 Lh^{-1}, aspiration rate 100% and solution feed rate 5 $mLmin^{-1}$. The inlet temperatures were fixed at 70 and 130°C for organic solvents and water, respectively. The outlet temperatures were in the range 50–55°C. The resulting solids were analysed by DSC and PXRD.

Milling of THF and THF-SAC Cocrystals

The THF-SAC cocrystals were prepared using a slurry crystallisation method prior to grinding. A mixture of THF (5.4 g) and SAC (5.49 g) was slurried in 30 mL of methanol for 4 days at room temperature. The suspension was then filtered under vacuum and dried at room temperature.

About 1 g of THF or THF-SAC was placed in a 10-mL grinding jar consisting of two steel balls and ground for 15 min in a Retsch grinder (Mixer Mill MM301, Retsch GmbH & Co., Germany) at 30-Hz oscillations. The powder was then collected, and the physical purity was verified by DSC and PXRD.

Differential Scanning Calorimetry

Thermal analyses of the samples were carried out on a DSC Q1000 (TA instrument) which was calibrated for temperature and enthalpy using indium. Samples (1–3 mg) were crimped in non-hermetic aluminum pans and scanned from 30 to 300°C at a heating rate of 10°C/min under a continuously purged dry nitrogen atmosphere (flow rate, 50 mL/min). The instrument was equipped with a refrigerated cooling system. The data were collected in triplicate for each sample.

Powder X-ray Diffraction

The solid phases were analysed by PXRD, and the resulting diffraction patterns were compared with the diffraction patterns of the pure phases. The patterns were collected on a Siemens DIFFRACplus 5,000 powder diffractometer with Cu Kα radiation (1.54056 Å). The tube voltage and amperage were set at 40 kV and 40 mA, respectively. The divergence slit and anti-scattering slit settings were variable for illumination of the 20-mm area of the sample. Each sample was scanned between 5 and 40°2θ, with a step size of 0.02° at 1 s/step. The sample stage was spun at 30 rpm. The instrument was pre-calibrated using a silicon standard.

Particle Size Analysis

An Aerosizer LD (TSI Incorporated, USA) sensor unit was used for the determination of particle size and particle size distributions (PSDs). All runs were carried out using more

System	Solvent used in spray drying	Drug/coformer stoichiometry	Total solution concentration (M)
THF	Methanol	1:0	0.02
THF-SAC	Methanol	1:1	0.02
THF-URE	Methanol	1:1	0.02
THF-NIC	Water	1:1	0.02

than 25,000 particles. The particle median diameter (MD) was calculated by the software.

Scanning Electron Microscopy

The qualitative particle size and morphology were observed under scanning electron microscopy (SEM, JSM 6460lv, JEOL, Japan). The samples were sprinkled onto double-sided tape that had been secured onto an aluminium stub and then gold sputter-coated under an argon atmosphere.

Inverse Gas Chromatography

Pre-silanised glass columns (300×4 mm ID) were packed with an appropriate mass of the powder and then plugged with silanised glass wool at both ends. Inverse gas chromatography (IGC) experiments were performed using an SMS-IGC 2000 (Surface Measurement Systems Ltd., London, UK) system. The packed column was pre-conditioned at 303 K and 0% relative humidity for 3 h. A series of pure n-alkane vapour probes (decane, nonane, octane, hexane and heptane) and polar probes (ethanol, ethyl acetate and acetonitrile) was injected at infinite dilution of 3% p/po, where p and po are the partial pressure and the vapour pressure at identical conditions, respectively. The corrected retention volume was determined using peak maximum analysis. Methane gas was used as a non-interacting probe at a concentration of 0.10 p/po. Helium was used as the carrier gas at a flow rate of 10.0 cm^3/min. Two columns of each sample were analysed, and three measurements per column were performed for every sample. Raw data were analysed using IGC Analysis Macros (v1.3 standard edition, Surface Measurement Systems, London, UK) according to the Schultz *et al.* (19) method.

For measuring the dispersive surface energy of the solid powder (γ_S^d), the retention volume (V_N) of each alkane was calculated from the following relationship:

$$V_N = jF(t_R - t_0)\frac{T}{273.15} \tag{1}$$

where j is the James–Martin pressure drop correction factor, F is the exit flow rate measured at 1 atm and 273.15 K, t_R is the retention time of the interacting probe, t_0 is the mobile phase hold up and T is the column temperature in degrees Kelvin. The net retention volume is related to the dispersive surface free energy component by

$$RT \ln V_N = 2N_A \left(\gamma_S^d\right)^{1/2} a_m \left(\gamma_L^d\right)^{1/2} + K \tag{2}$$

where R is the universal gas constant, N_A is Avogadro's number, a_m is the cross-sectional area of the adsorbate, γ_L^d is the dispersive surface tension of the probe and K is a constant.

Equation 2 is a linear relationship where γ_S^d can be calculated from the slope of the line.

The polar components can be evaluated from the retention behaviour of the polar probes from the following relationship (assuming that the entropic contribution to the free energy is negligible (4)):

$$\Delta G^{AB} = K_A \text{DN} + K_D \text{AN}^* \tag{3}$$

where ΔG^{AB} is the free energy of adsorption of a polar probe on a solid material, DN is an electron donor or base parameter, and AN* is an electron acceptor or acid parameter. Ethanol (acidic), ethyl acetate (basic) and acetonitrile (basic) were used as polar probe molecules.

A linear plot of $\Delta G^{AB}/\text{AN}^*$ *versus* DN/AN^* was obtained by measuring the value of ΔG^{AB} for the polar probes. The Gutmann acidity constant K_A and basicity constant K_D of the sample powders were then determined from the slope and the intercept of the line, respectively.

In Vitro Aerosol Performance

The inhalation behaviour of spray-dried THF and its cocrystals (THF-NIC, THF-URE and THF-SAC) was characterised using drug-alone (carrier-free) and drug-carrier dry powder inhaler (DPI) formulations in an Aerolizer® inhaler device. A next-generation impactor (NGI, MSP Corp., Shoreview, MN) was used to assess drug-alone formulations, and a multi-stage liquid impinger (Copley Scientific, UK) was used to assess drug-carrier formulations.

For drug-alone formulations, about 10 mg of each powder was manually filled into size 3 HPMC capsules. The NGI pans were coated with a film of silicon oil to eliminate bounce and re-entrapment of particles. The capsules were placed into an Aerolizer® inhaler device, pierced and actuated into the NGI through a stainless steel USP throat adapter at a flow rate of 60 L/min for 6 s.

Ten capsules were tested for every formulation. After ten actuations, the powders were reconstituted from the capsules, the device and the NGI plates using water, except for THF-SAC cocrystals where methanol is used. Each experiment was repeated twice. The collected samples were analysed by high-performance liquid chromatography (HPLC; 1260, Agilent, USA). Theophylline was separated on a C8 column (5 μm, 150×4.6 mm). The HPLC analysis was conducted at 40°C with a flow rate of 1 mL/min. The UV detection was at 273 nm, and the mobile phase was 0.1% *w/v* trifluoroacetic acid in water/methanol in proportions of 75:25.

The drug-carrier formulations were prepared by mixing drug particles [50 mg each of spray-dried (SD)-THF, SD-THF-

NIC, SD-THF-URE and SD-THF-SAC] with carrier particles (2 g of α-lactose monohydrate, characterised in detail elsewhere under standard conditions (Turbula® mixer: Willy A. Bachofen AG, Basel, Switzerland, 100 rpm and 30 min mixing time) to prepare a 2.5% drug-carrier system for all the formulations (37). After blending, 40±1 mg of each formulation powder was filled manually into hard gelatine capsules (size 3) so that each capsule contained 10±0.3 mg of drug. Pharmacopoeial deposition experiments were performed as described in detail elsewhere (38), except for the THF-SAC cocrystals where methanol was used instead of water. Each deposition experiment involved the actuation of ten capsules and was repeated three times. Several parameters were employed to characterise the deposition profiles of the formulations under investigation; these included recovery (RE), mass median aerodynamic diameter (MMAD), geometric standard deviation (GSD), impaction loss (IL) and fine particle fraction (FPF$_{\leq 5\mu m}$), which were calculated as described previously (38). Drug loss (DL, defined as the ratio of the amount of drug remaining in the capsule shells, inhaler and mouthpiece adaptor to the RD, as a percentage) was also calculated, where RD is the sum the amounts of drug remained in capsules, inhaler device and deposited on throat and all stages of the impactor. It is important to note that the powders of THF-SAC, -URE and THF-NIC contained 50, 75 and 60 wt% of THF, respectively; the rest of the weight was contributed by the conformers.

Statistical Analysis

One-way analysis of variance was applied (where appropriate) to compare results in this study. *P* values less than 0.05 were considered as indicative of statistically significant difference.

RESULTS AND DISCUSSION

Preparation of the Materials and Their Phase Purity

Table II lists the characteristics of the cocrystals and THF form I used in this study. The crystal structures of THF-URE and THF-SAC cocrystals have been reported previously

(34,35). As can be seen, the structural features (special groupings and lattice parameters) of these cocrystals and THF form I are considerably different (Table II). The crystal structure of THF-NIC cocrystals has not yet been reported; however, complete solid-state characterisation is available (36).
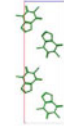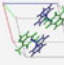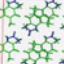
The cocrystals of theoyphylline with URE and NIC were found to be incongruently saturating in methanol and water, respectively, whereas THF-SAC cocrystal is congruently saturating in methanol. The spray drying method was demonstrated as a suitable method for preparing pure cocrystal systems for incongruently saturating systems in our laboratory. Spray drying method provides flexibility with the choice of solvents and the prior knowledge of cocrystals phase diagrams shown to be less important as compared to slurry crystallization method. Adequate control over the solid-state and particle properties can be achieved concurrently with spray drying (27). Feed solutions of various samples were prepared as presented in Table I and spray dried. The powders were collected, and the phase purity was examined by DSC and PXRD. DSC showed a single melting point for the cocrystals, which corroborates with available previous reports (Electronic Supplementary Material) (36).

PXRD patterns for spray-dried materials (Fig. 1) had also matched previously reported and/or simulated patterns, confirming the physical purity of the spray-dried powders (34,35). This demonstrates once again the capability of spray drying in making pure cocrystal phases even for the incongruently saturating systems. Figure 1 shows the overlaid PXRD patterns of THF in received form and THF-SAC cocrystals prepared by slurry method- milled and spray-dried powders. All these samples were confirmed to be physically pure and crystalline.

Characterization of Particle Size and Morphology

It is well known that the particle size and morphology of a powder can have a profound effect on its aerosol performance in DPIs (37). Figure 2a shows that the PSD for the spray-dried cocrystals varied considerably. These differences might have had a considerable effect on the DPI performance. Most of the cocrystal particles were smaller than 5 μm, as also seen in the SEM pictures (Fig. 2c–f), which makes them suitable for

Table II. Theophylline and the Cocrystals Used in the Study with their Abbreviations, Stoichiometric Ratio, CSD REFCODE and Spacial Grouping

Solid form	Abbreviation	Drug/Coformer molar ratio	Saturation condition	Unit cell viewed along b* axis	CSD REFCODE (space group)
Theophylline anhydrous	THF	1:0	NA		BAPLOT01 (Pna21)
Theophylline-Saccharin	THF-SAC	1:1	congruent		XOBCUN (P-1)
Theophylline-Urea	THF-URE	1:1	incongruent		DUXZAX (C2/c)
Theophylline-Nicotinamide	THF-NIC	1:1	incongruent	N/A	N/A

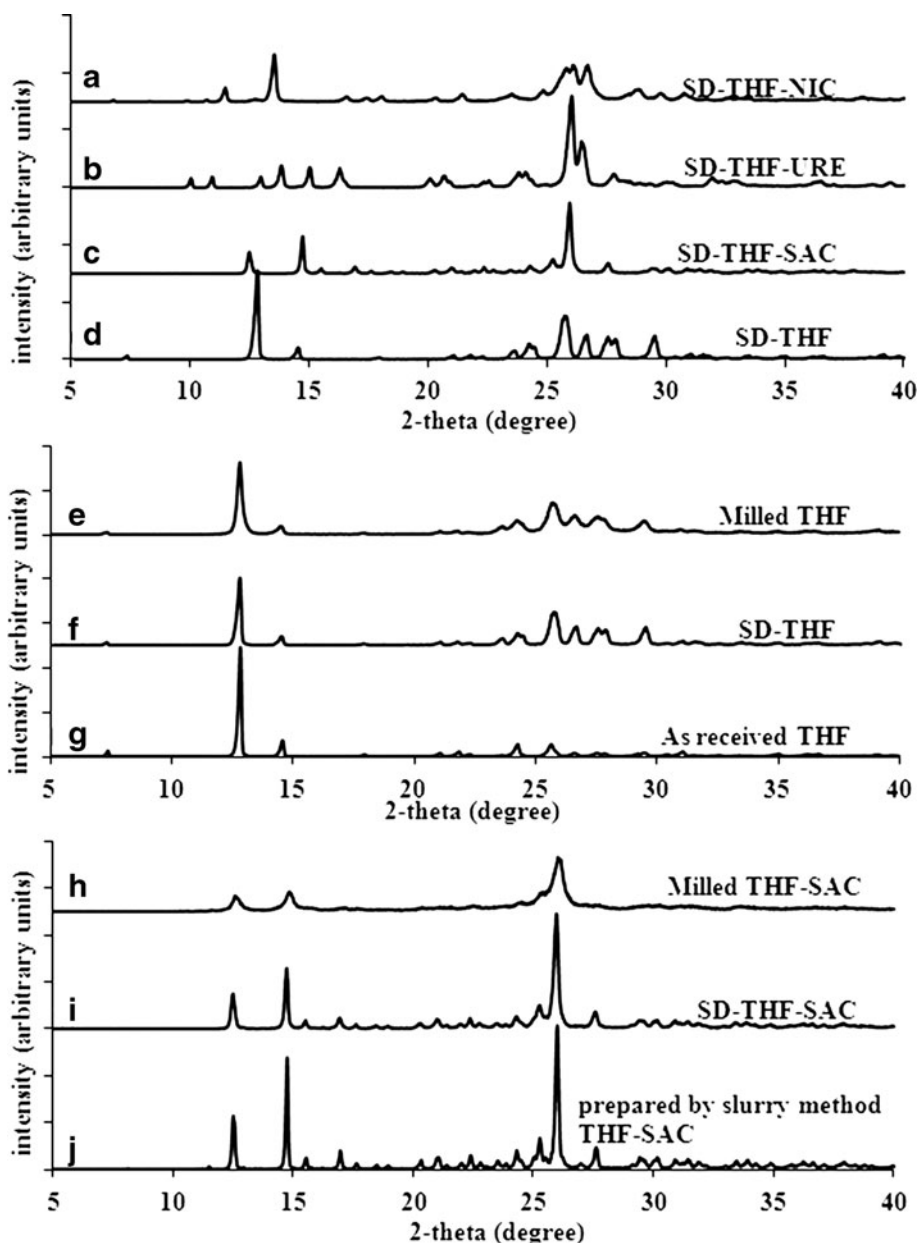The green and blue molecules are theophylline and conformer, respectively

Fig. 1. Powder X-ray diffraction patterns (PXRD) for **a** SD-THF-NIC, **b** SD-THF-URE, **c** SD-THF-SAC, **d** SD-THF, **e** milled THF, **f** SD-THF, **g** as-received THF, **h** milled THF-SAC, **i** SD-THF-SAC, **j** prepared by slurry method THF-SAC

pulmonary drug delivery. However, the SEM images indicate that the spray-dried cocrystals were assembled as clusters with varying degrees of agglomeration (Fig. 2c–f), which could possibly result in variations in powder aerosol behaviour and performance (4). These agglomeration characteristics can be attributed to cohesion between the particles, as is inherent to spray-dried fine particulate drugs. The agglomerates could be loose as discrete fine particles were observed distributed across the larger agglomerates (Fig. 3a, b). The median diameter of the spray-dried cocrystal particles was ranked in the following order: THF≈THF-NIC<THF-URE<THF-SAC (Fig. 2b).

The morphology of the spray-dried particles was observed using high-resolution SEM. A striking difference was

observed between THF and the THF cocrystals (Fig. 3). SD-THF particles were elongated (tubular or acicular; Fig. 3a), whereas SD-THF-URE cocrystal particles were flakes (plate-like) and were agglomerated with a fractured (network-like) surface morphology (Fig. 3c). SD-THF-NIC (Fig. 3b) and SD-THF-SAC (Fig. 3d) cocrystal particles were irregular (de-formed) in shape. The variations in particle morphology among SD-THF, SD-THF-URE and SD-THF-SAC cocrystals despite similar processing conditions during spray drying can be explained by the considerable differences in the crystalli-zation kinetics and/or crystal lattices (26,28). Thus, cocrystal-lization could be considered as a potential particle-engineering technique. Figure 4 shows the morphology of THF and THF-SAC cocrystals before and after milling; all
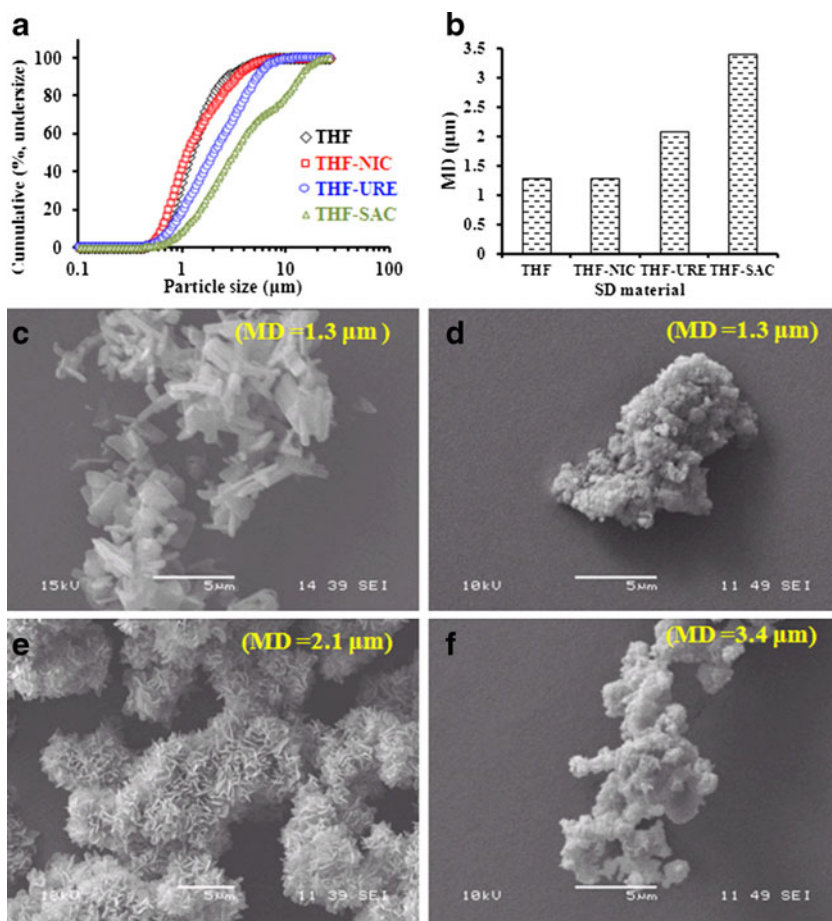
Fig. 2. Cumulative (percentage, undersize) particle size distribution **a**, median diameter (MD) **b**, and SEM pictures **c**, **d**, **e**, **f** for spray-dried (SD)-THF and the cocrystals SD-THF-NIC, SD-THF-URE and SD-THF-SAC

the particles are irregular. The PSDs of both milled materials were comparable (Fig. 4), and in a similar range to those of SD-THF and the SD-THF-SAC cocrystals (Fig. 2a), showing a unimodel distribution curve.
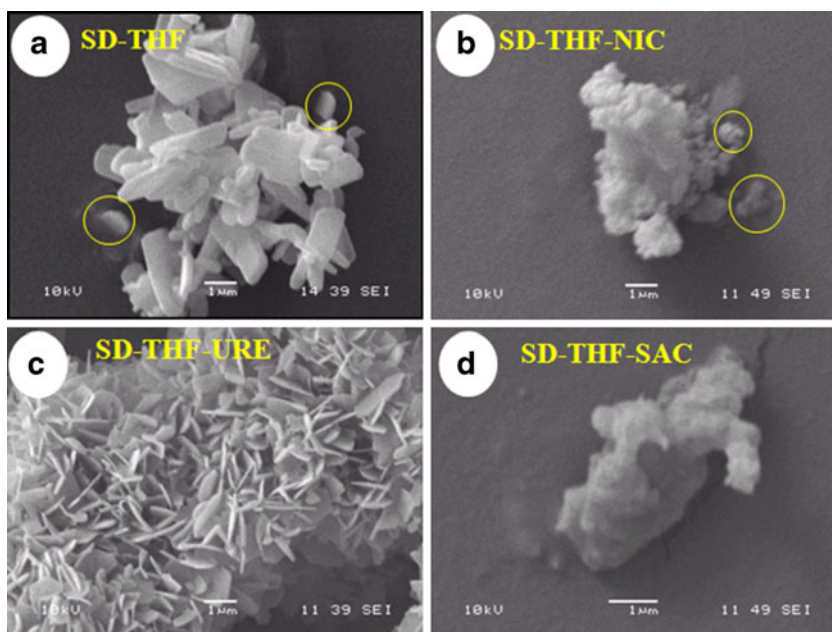

Fig. 3. SEM pictures of **a** SD-THF, and the cocrystals: **b** SD-THF-NIC, **c** SD-THF-URE and **d** SD-THF-SAC
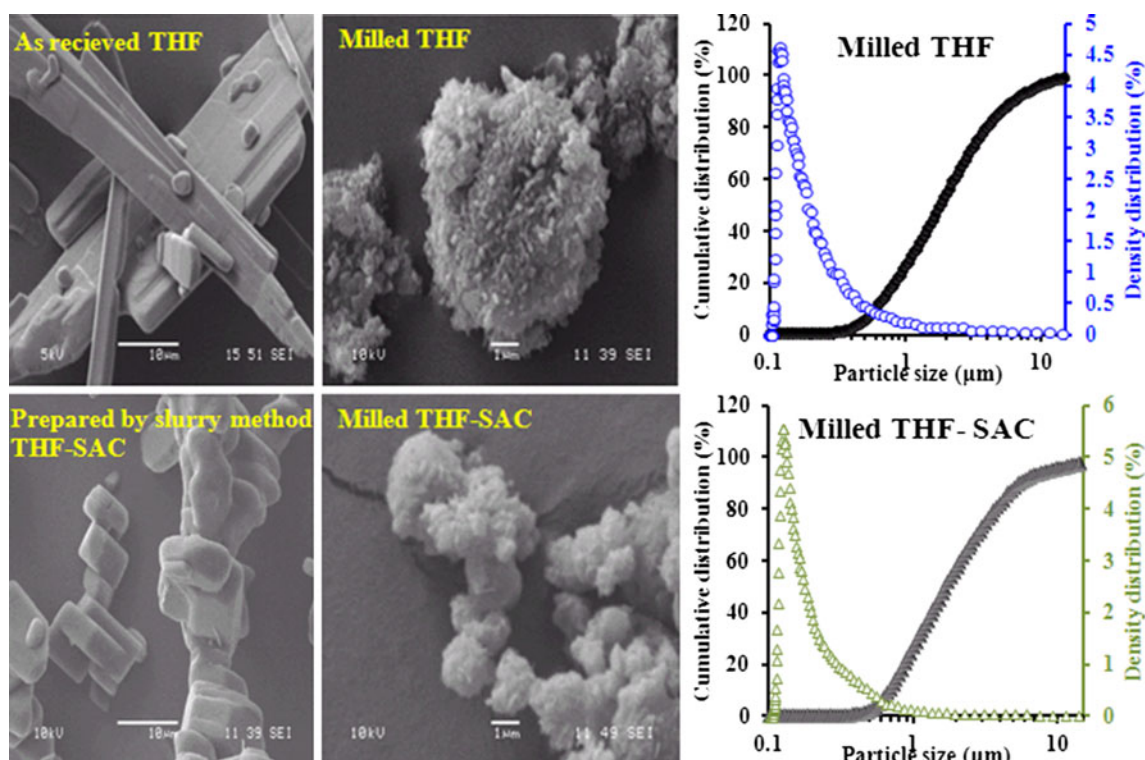
Fig. 4. SEM photographs of the following samples: THF (as received), THF-SAC (prepared by slurry method), milled THF and milled THF-SAC, along with the particle size distribution of milled THF and milled THF-SAC

Surface Energy of Spray-Dried and Milled Samples

Changes in the solid form and crystal habit of a material can lead to changes in its surface chemistry and surface energy (39–42). The dispersive surface energies of the spray-dried cocrystals were ranked in the following order ($P<0.05$): SD-THF < SD-THF-URE < SD-THF-SAC < SD-THF-NIC (Fig. 5a). The dispersive surface energy of the SD-THF-NIC particles was remarkably different from that of the other powders, possibly because of differences in the crystals' structure resulting from different chemical functionalities on the dominant facets. The dispersive energy of SD-THF-URE was only marginally different, despite obvious differences in solid form and morphology (Figs. 2e and 3c). Thus, particles with
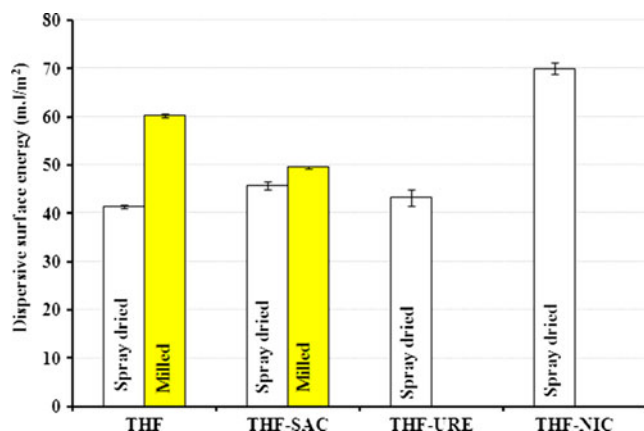

Fig. 5. Dispersive surface energy for spray-dried drug and cocrystals and milled THF and THF-SAC cocrystals

different solid forms and/or different crystal habits can have different surface energies. Similar observations were made for ibuprofen in a previous study (15).

The basicity constant (K_D) was not significantly different from zero for all the spray-dried materials (Table III). In contrast, the acidity constant (K_A) for the spray-dried cocrystal particles varied considerably: SD-THF-NIC > SD-THF-URE > SD-THF-SAC = SD-THF (Table III). The specific free energy (ΔG^{AB}) for the acidic probe, ethanol, was lower than that for the basic probes, ethyl acetate and acetonitrile, for all the powders (Table III), indicating that the powders were more acidic or electron accepting in nature. ΔG^{AB} (Table III) was highest for SD-THF-NIC, indicating that the surface of this powder was the most acidic in nature.

Generally, the dispersive surface energy and K_A were higher for milled particles than for spray-dried particles (Fig. 5b). Moreover, ΔG^{AB} for the acid probe was lower than ΔG^{AB} for the basic probes (Table III), which indicates a more electron-accepting tendency for the milled surfaces. Similarly, ΔG^{AB} values for the basic probes were higher for the milled samples than for the spray-dried samples (Table III), which is indicative of the more acidic nature of the milled surfaces. Interestingly, the milled THF samples had a higher surface energy than the milled THF-SAC cocrystals, while the opposite trend was seen for SD-THF and SD-THF-SAC cocrystals (Table III). This may have been due to the exposure of different facets and/or acidic functional groups on the material surface after processing. The effects of processing on the surface energies of different materials have been previously investigated (43–46). For example, milled lactose has a higher dispersive surface energy than spray-dried

Table III. The Surface Energy Parameters of Different Samples Determined Using IGC

Material	γ^d (mJ/m^2)	K_A	K_D	ΔG^{AB} (KJ/mol)		
				Ethanol	Acetonitrile	Ethyl acetate
SD-THF	41.39±0.42	0.13±0.00	0.02±0.00	7.48±0.4	10.47±0.05	9.63±0.66
SD-THF-SAC	45.70±0.79	0.13±0.00	0.00	5.71±0.14	7.80±0.25	8.94±0.28
SD-THF-Urea	43.23±1.71	0.15±0.00	0.00	8.60±0.12	9.15±0.14	10.28±0.04
SD-THF-NIC	69.98±1.23	0.16±0.00	0.00	9.36±0.36	11.27±0.22	11.48±0.09
Milled THF	60.26±0.42	0.16±0.01	0.00	7.95±1.32	10.93±2.27	11.38±0.61
Milled THF-SAC	49.58±0.20	0.16±0.05	0.00	6.79±0.02	8.96±0.04	10.76±0.12

Results are presented as averages±standard deviations for two columns, with three runs per column for each sample

particles (47). In fact, the acidic nature of the milled lactose was attributed in another study to the increased presence of hydroxyl groups on the surface (48).

Aerosol Performance of Spray-Dried Cocrystal Particles

The aerodynamic particle size distribution for drug-alone and drug-carrier DPI formulations was larger than the aerodynamic particle size for the spray-dried materials obtained by

time of flight, demonstrating that the drug particles were not dispersed into individual particles (Fig. 6). In theory, this could be attributed to either drug–drug agglomeration (high drug–drug cohesion) or insufficient drug-carrier deaggregation (higher drug-carrier adhesion) (49). For the SD-THF-URE and SD-THF-SAC cocrystals, drug-carrier aerosol formulations generated larger aerodynamic size of THF than drug-alone aerosol formulations which in turn generated THF particles with larger size than primary geometric size distribution
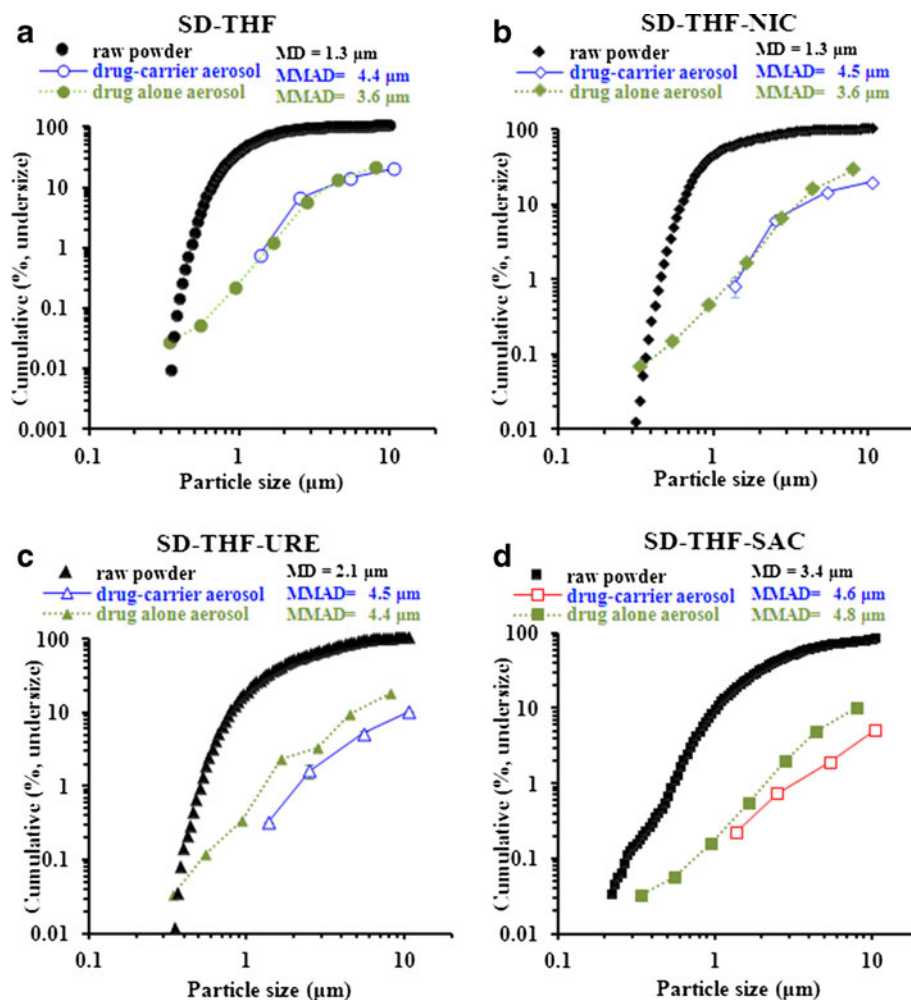

Fig. 6. Comparison of particle size distribution of spray-dried (SD)-THF and the cocrystals SD-THF-NIC, SD-THF-URE and SD-THF-SAC before aerosolization (raw powder) and after aerosolization from drug-alone and drug-carrier aerosols
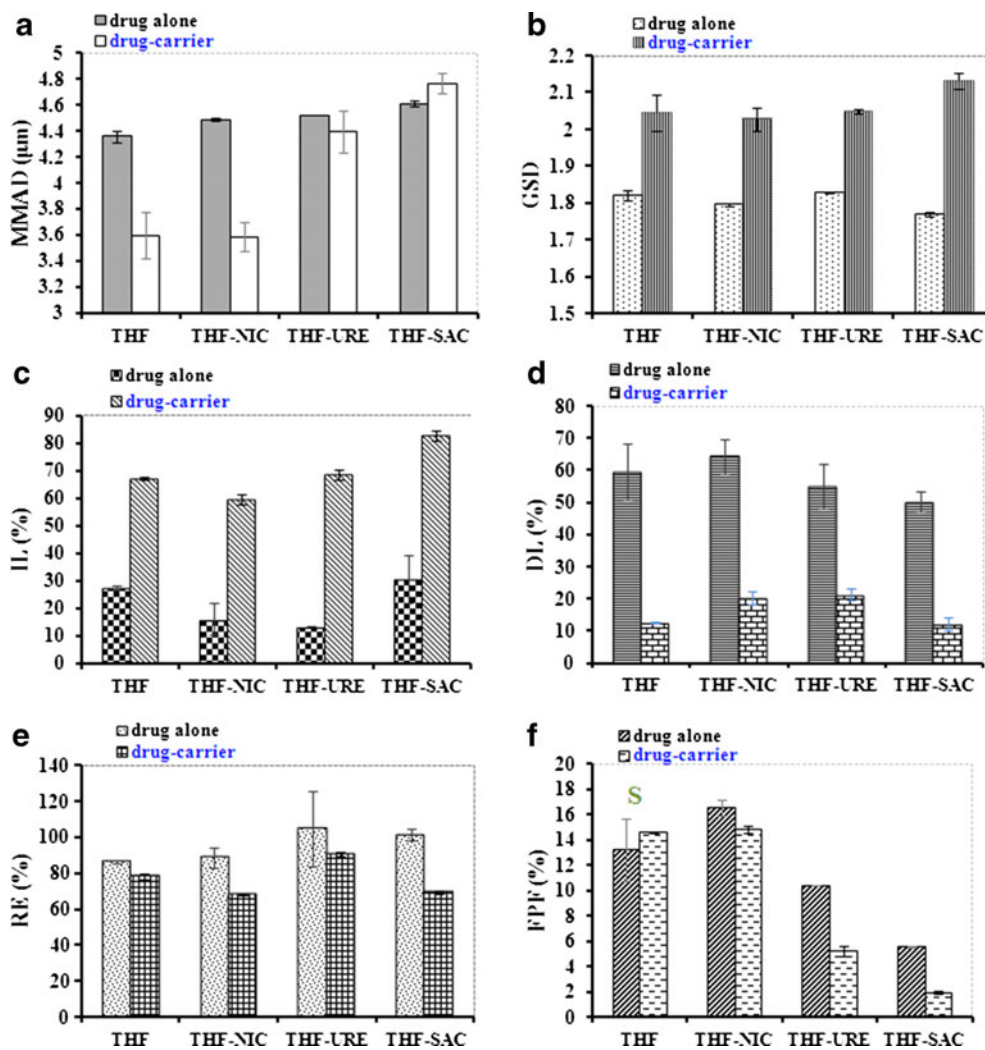
Fig. 7. Mass median aerodynamic diameter (MMAD) **a**, geometric standard deviation (GSD) **b**, impaction loss (IL) **c**, drug loss (DL) **d**, percentage recovery (RE) **e** and fine particle fraction (FPF) obtained from drug-alone and drug-carrier formulations containing spray-dried (SD)-THF and the cocrystals: SD-THF-NIC, SD-THF-URE and SD-THF-SAC. *S* indicates statistically similar ($P>0.05$)

(Fig. 6c, d). This indicates that SD-THF-URE and SD-THF-SAC particles in drug-carrier aerosols were not sufficiently dispersed to individual drug particles during inhalation.

The MMAD for the spray-dried cocrystal particles, which varied considerably, was ranked in the following order: THF ≤ THF-NIC<THF-URE<THF-SAC (Fig. 7a). For THF and THF-NIC, the MMAD obtained from the drug-alone aerosols
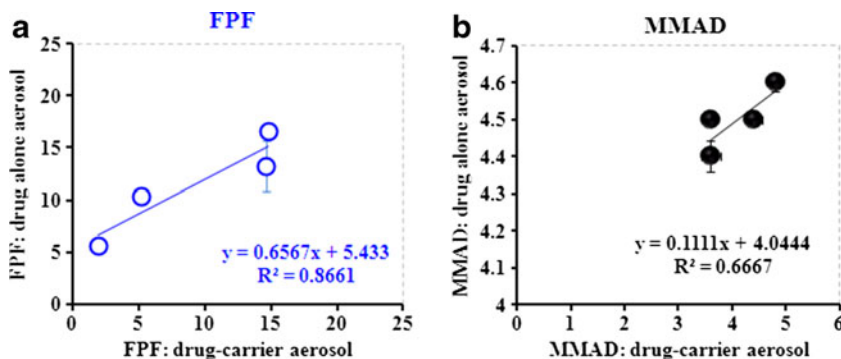

Fig. 8. Fine particle fraction (FPF) **a** and mass median aerodynamic diameter (MMAD) **b** obtained from drug-alone aerosols in relation to deposition parameters obtained from drug-carrier aerosols

was considerably higher than that obtained from the drug-carrier aerosols (Fig. 7a), which is indicative of a higher degree of agglomeration.

Also, all drug-alone formulations generated higher GSDs than the drug-carrier formulations (Fig. 7b). This indicates less particle size polydispersity for the drug-carrier aerosols, which is considered advantageous in DPI systems.

In comparison to the drug-carrier formulations, the drug-alone (carrier-free) formulations generated a considerably lower IL (Fig. 7c). The higher DL for drug-alone aerosols (Fig. 7f) indicates more particle agglomeration, which is in agreement with the MMAD data.

All the drug-carrier aerosols containing SD-THF cocrystals (but not those with SD-THF itself) had smaller REs (Fig. 7e) and smaller FPFs (Fig. 7f) than the drug-alone aerosols. This indicates that spray-dried aerosol particles from

drug-alone formulations outperformed spray-dried aerosol particles from drug-carrier formulations. These results could be attributed to the high degree of drug-carrier adhesion, as confirmed by the relatively high IL generated from all drug-carrier aerosols (60–83%, Fig. 7c).

Regardless of formulation type (drug-alone or drug-carrier), the FPFs were ranked in the following order: SD-THF≈SD-THF-NIC>SD-THF-URE>SD-THF-SAC (Fig. 7f). Based on these data (Fig. 7f) and the aerodynamic size distributions (Fig. 6), it can be concluded that the SD-THF and SD-THF-NIC aerosols performed best, while the SD-THF-SAC aerosols were worst.

Interestingly, linear relationships were established when plotting FPF (r^2=0.8661, Fig. 8a) or MMAD (r^2=0.7257, Fig. 8b) data for drug-alone *versus* drug-carrier formulations. These relationships reflect reasonably good agreement between the aerosol formulations in terms of inhalation performance.

Variations between different spray-dried materials in terms of aerosol efficiency could be attributed to their different physicochemical properties, as discussed previously. The results showed that FPF increased with decreasing particle median size (Fig. 9a) and decreasing particle experimental aerodynamic diameter (Fig. 9b). Except for THF-NIC cocrystal, spray-dried cocrystals with smaller surface energy generated higher FPF upon aerosolization (Fig. 9c). Statistical correlation analysis indicated that particle micromeritic properties such as particle size (geometrical or MMAD) are more important than particle surface energy in determining drug aerosol performance from DPIs. Nevertheless, it should be kept in mind that there is a high probability of interaction between the different drug physical parameters (e.g. size, morphology, surface energy, *etc.*) which unfortunately could not be limited (more than one parameter was varied). More effort is required to study to study the influence of drug surface properties on drug aerosolization performance in case of drug particles with similar micrometric properties.

Fig. 9. Fine particle fraction (FPF) in relation to particle median diameter (MD) **a**, experimental mass median aerodynamic diameter (MMAD) **b** and surface energy (γ^d) **c** (means±SD, $n \geq 2$)

CONCLUSIONS

It was possible to prepare highly crystalline cocrystals of THF by spray drying with different particle characteristics. In comparison to milled theophylline cocrystals, novel spray-dried cocrystals demonstrated considerably smaller surface energies. Also, the cocrystals of THF prepared by spray drying showed different micromeritic properties, demonstrating the potential of cocrystallization technology to control particle physicochemical properties. The milled materials were more acidic and had higher surface energies than the spray-dried materials. The precise interrelationship between drug physical properties, carrier physical properties and drug powder inhaler formulation performance remains obscure. However, this study suggested that cocrystal particle micromeritic properties are more important than particle surface energy in terms of determining aerosolization behaviour. Therefore, the drug particle surface energy alone may not predict drug *in vitro* aerosolization performance. However, it should be kept in mind that milling has generated unbalanced high surface energy, whereas minimized surface energy was obtained in the case of spray drying. Further work would be warranted to
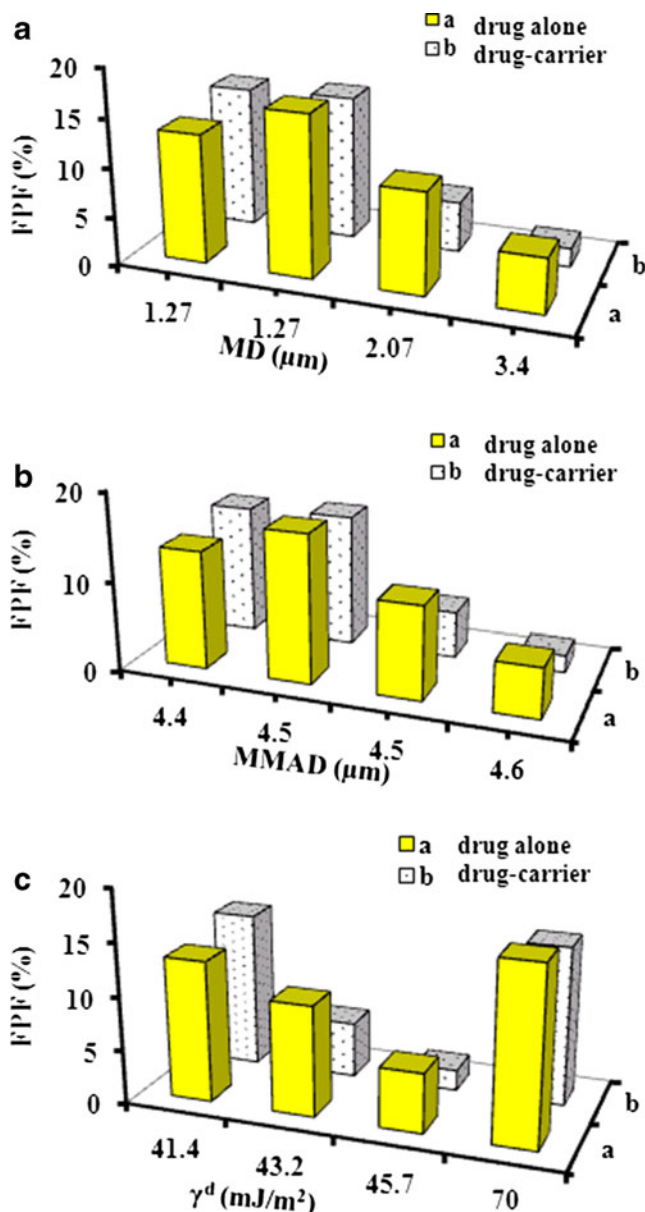
investigate if spray drying could be applied as an efficient technique to prepare cocrystals other than theophylline.

REFERENCES

1. Begat P, Morton D, Staniforth J, Price R. The cohesive-adhesive balances in dry powder inhaler formulations I: direct quantification by atomic force microscopy. Pharm Res. 2004;21:1591–7.
2. Paajanen M, Katainen J, Raula J, Kauppinen E, Lahtinen J. Direct evidence on reduced adhesion of salbutamol sulphate particles due to L-leucine coating. Powder Technol. 2009;192:6–11.
3. Zeng X, Martin G, Tee S, Ghoush A, Marriott C. Effects of particle size and adding sequence of fine lactose on the deposition of salbutamol sulphate from a dry powder formulation. Int J Pharm. 1999;182:133–44.
4. Gutmann V. The donor–acceptor approach to molecular interactions. New York: Plenum Press; 1978.
5. Feeley J, York P, Sumby B, Dicks H. Determination of surface properties and flow characteristics of salbutamol sulphate, before and after micronisation. Int J Pharm. 1998;172:89–96.
6. Begat P, Young P, Edge S, Kaerger J, Price R. The effect of mechanical processing on surface stability of pharmaceutical powders: visualization by atomic force microscopy. J Pharm Sci. 2003;92:611–20.
7. Fowkes FM. Attractive forces at interfaces. Ind Eng Chem. 1964;56:40–52.
8. Van Oss C, Good R, Chaudhury M. Additive and nonadditive surface tension components and the interpretation of contact angles. Langmuir. 1988;4:884–91.
9. Van Oss C. Acid–base interfacial interactions in aqueous media. Colloids Surf, A Physicochem Eng Asp. 1993;78:1–49.
10. Buckton G. The estimation and application of surface energy data for powdered systems. Drug Dev Ind Pharm. 1992;18:1149–67.
11. Buckton G, Gill H. The importance of surface energetics of powders for drug delivery and the establishment of inverse gas chromatography. Adv Drug Deliv Rev. 2007;59:1474–9.
12. Ahfat NM, Buckton G, Burrows R, Ticehurst MD. An exploration of inter-relationships between contact angle, inverse phase gas chromatography and triboelectric charging data. Eur J Pharm Sci. 2000;9:271–6.
13. Pinto J, Buckton G, Newton J. A relationship between surface free energy and polarity data and some physical properties of spheroids. Int J Pharm. 1995;118:95–101.
14. Alhalaweh A, Vilinska A, Gavini E, Rassu G, Velaga SP. Surface thermodynamics of mucoadhesive dry powder formulation of zolmitriptan. AAPS PharmSciTech. 2011;12(4):1186–92.
15. Grimsey IM, Feeley JC, York P. Analysis of the surface energy of pharmaceutical powders by inverse gas chromatography. J Pharm Sci. 2002;91:571–83.
16. Chiou D, Langrish T. A comparison of crystallisation approaches in spray drying. J Food Eng. 2008;88:177–85.
17. Basavoju S, Boström D, Velaga S. Indomethacin-saccharin cocrystal: design, synthesis and preliminary pharmaceutical characterization. Pharm Res. 2008;25:530–41.
18. Jung M, Kim J, Kim M, Alhalaweh A, Cho W, Hwang S, et al. Bioavailability of indomethacin saccharin cocrystals. J Pharm Pharmacol. 2010;62:1560–8.
19. Schultheiss N, Newman A. Pharmaceutical cocrystals and their physicochemical properties. Cryst Growth Des. 2009;9:2950–67.
20. Alhalaweh A, George S, Bostrom D, Velaga SP. 1:1 and 2:1 Urea–succinic acid cocrystals: structural diversity, solution chemistry, and thermodynamic stability. Cryst Growth Des. 2010;10:4847–55.
21. Alhalaweh A, Sokolowski A, Rodriguez-Hornedo N, Velaga SP. Solubility behavior and solution chemistry of indomethacin cocrystals in organic solvents. Cryst Growth Des. 2011;11:3923–9.
22. Nehm S, Rodriguez-Spong B, Rodriguez-Hornedo N. Phase solubility diagrams of cocrystals are explained by solubility product and solution complexation. Cryst Growth Des. 2006;6:592–600.
23. Mohammad MA, Alhalaweh A, Velaga SP. Hansen solubility parameter as a tool to predict cocrystal formation. Int J Pharm. 2011;407:63–71.
24. Alhalaweh A, George S, Basavoju S, Childs SL, Rizvi SAA, Velaga SP. Pharmaceutical cocrystals of nitrofurantoin: screening, characterization and crystal structure analysis. Cryst Eng Comm. 2012;14:5078–88.
25. Alhalaweh A, Roy L, Rodríguez-Hornedo N, Velaga SP. pH-dependent solubility of indomethacin-saccharin and carbamaze-pine-saccharin cocrystals in aqueous media. Mol Pharmaceut. 2012. doi:10.1021/mp300189b.
26. Cassidy A, Gardner C, Jones W. Following the surface response of caffeine cocrystals to controlled humidity storage by atomic force microscopy. Int J Pharm. 2009;379:59–66.
27. Vehring R. Pharmaceutical particle engineering via spray drying. Pharm Res. 2008;25:999–1022.
28. Alhalaweh A, Velaga S. Formation of cocrystals from stoichiometric solutions of incongruently saturating systems by spray drying. Cryst Growth Des. 2010;10:3302–5.
29. Suzuki E, Shimomura K, Sekiguchi K. Thermochemical study of theophylline and its hydrate. Chem Pharm Bull. 1989;37:493–7.
30. Phadnis NV, Suryanarayanan R. Polymorphism in anhydrous theophylline—implications on the dissolution rate of theophylline tablets. J Pharm Sci. 1997;86:1256–63.
31. Debnath S, Suryanarayanan R. Influence of processing-induced phase transformations on the dissolution of theophylline tablets. AAPS PharmSciTech. 2004;5:39–49.
32. Seton L, Khamar D, Bradshaw IJ, Hutcheon GA. Solid state forms of theophylline: presenting a new anhydrous polymorph. Cryst Growth Des. 2010;10(9):3879–86.
33. Jayasankar A. Understanding the mechanisms, thermodynamics and kinetics of cocrystallization to control phase transformations: The University of Michigan; 2008.
34. Wiedenfeld H, Knoch F. Arch Pharmacal Res. 1986;319:654–9.
35. Lu E, Rodríguez-Hornedo N, Suryanarayanan R. A rapid thermal method for cocrystal screening. Cryst Eng Comm. 2008;10:665–8.
36. Lu J, Rohani S. Preparation and characterization of theophylline-nicotinamide cocrystal. Org Process Res Dev. 2009;13:1269–75.
37. Kaialy W, Ticehurst MD, Murphy J, Nokhodchi A. Improved aerosolization performance of salbutamol sulfate formulated with lactose crystallized from binary mixtures of ethanol–acetone. J Pharm Sci. 2011;100:2665–84.
38. Trask AV, Motherwell W, Jones W. Physical stability enhancement of theophylline via cocrystallization. Int J Pharm. 2006;320:114–23.
39. Hooton JC, German CS, Davies MC, Roberts CJ. A comparison of morphology and surface energy characteristics of sulfathiazole polymorphs based upon single particle studies. Eur J Pharm Sci. 2006;28:315–24.
40. Sheth A, Grant D. Relationship between the structure and properties of pharmaceutical crystals. Kona. 2005;23:36–48.
41. Bethune S, Huang N, Jayasankar A, Rodri guez-Hornedo N. Understanding and predicting the effect of cocrystal components and pH on cocrystal solubility. Cryst Growth Des. 2009;9:3976–88.
42. Tong HHY, Shekunov BY, York P, Chow AHL. Influence of polymorphism on the surface energetics of salmeterol xinafoate crystallized from supercritical fluids. Pharm Res. 2002;19:640–8.
43. Heng JYY, Thielmann F, Williams DR. The effects of milling on the surface properties of form I paracetamol crystals. Pharm Res. 2006;23:1918–27.
44. Shekunov BY, Feeley JC, Chow AHL, Tong HHY, York P. Aerosolisation behaviour of micronised and supercritically-processed powders. J Aerosol Sci. 2003;34:553–68.
45. Chamarthy SP, Pinal R, Carvajal MT. Elucidating raw material variability—importance of surface properties and functionality in pharmaceutical powders. AAPS PharmSciTech. 2009;10:780–8.

46. Lechuga-Ballesteros D, Charan C, Stults CLM, Stevenson CL, Miller DP, Vehring R, *et al*. Trileucine improves aerosol performance and stability of spray-dried powders for inhalation. J Pharm Sci. 2008;97:287–302.

47. Newell HE, Buckton G, Butler DA, Thielmann F, Williams DR. The use of inverse phase gas chromatography to measure the surface energy of crystalline, amorphous, and recently milled lactose. Pharm Res. 2001;18:662–6.

48. Tong HHY, Shekunov BY, York P, Chow AHL. Predicting the aerosol performance of dry powder inhalation formulations by interparticulate interaction analysis using inverse gas chromatography. J Pharm Sci. 2006;95:228–33.

49. Feeley J, York P, Sumby B, Dicks H. Processing effects on the surface properties of α-lactose monohydrate assessed by inverse gas chromatography (IGC). J Mater Sci. 2002;37:217–22.